

Comparison of h -, p - and hp -adaptation for convective heat transfer

D. W. Pepper & X. Wang

*Nevada Center for Advanced Computational Methods,
University of Nevada Las Vegas, USA*

Abstract

Three adaptive FEM algorithms based on mesh refinement (h -adaptation), mesh enrichment (p -adaptation) and the combination of both (hp -adaptation) are employed to solve incompressible fluid flow problems including convective heat transfer effects. Test cases of natural convection in a square cavity with different Rayleigh numbers are solved using primitive variables in a modified finite element approach employing the three adaptive strategies. Results show excellent agreement among benchmark data available in the literature.

Keywords: h -, p -, hp - adaptation, FEM, natural convection.

1 Introduction

The finite element method (FEM) is a popular numerical tool used in many heat transfer and fluid flow simulations. The FEM is capable of easily dealing with irregular geometries and has the ability to implement enhanced accuracy using general-purpose algorithms. Adaptive FEM is especially attractive since it can dynamically control mesh characteristics to obtain desired accuracy. Following early work using h -adaptive FEM to accurately capture shock waves in compressible flow [1], the adaptive FEM has become an active research area over the past decade.

Generally, there are four categories of adaptation: (1) h -adaptation, where the element sizes vary while the order of the shape functions are constant; (2) p -adaptation, where the order of the shape functions vary while the element sizes are constant; (3) r -adaptation, where the nodes are redistributed in an existing mesh in the process of adaptation while the total element and node number are



constant; (4) *hp*-adaptation, which is a combination of both *h*- and *p*- method. *hp*-adaptive schemes are among the best mesh based schemes with the potential payoff of achieving exponential converge rate [2, 3].

In this paper, three adaptive FEM algorithms based on mesh refinement (*h*-adaptation), mesh enrichment (*p*-adaptation) and the combination of both (*hp*-adaptation) are employed to solve incompressible fluid flow problems with convective heat transfer. Results are compared for different algorithms along with a brief discussion of computational efficiency.

2 Governing equations and solution procedure

The non-dimensional governing equations for incompressible laminar viscous fluid in a Boussinesq and constant property are written in the forms:

Continuity equation:

$$\nabla \cdot V = 0 \quad (1)$$

Conservation of Momentum

$$\frac{\partial V}{\partial t} + V \cdot \nabla V = -\nabla p + \text{Pr} \nabla^2 V + C_{grav} T \quad (2)$$

for the x-direction, $C_{grav} = 0$; for the y-direction, $C_{grav} = Ra \text{Pr}$. The energy equation can be written as

Energy equation

$$\frac{\partial T}{\partial t} + V \cdot \nabla T = \frac{1}{\text{Pe}} \nabla^2 T + Q \quad (3)$$

The following non-dimensional parameters are used to derive the above equations.

$$X = \frac{X^*}{L}, V = \frac{V^*}{\alpha/L}, p = \frac{p^*}{\rho \alpha^2 / L^2}, t = \frac{t^*}{L^2 / \alpha}, T = \frac{T^* - T_c}{T_h - T_c} \quad (4)$$

with the Rayleigh number, Prandtl number, and Peclet number defined as

$$Ra = \frac{g\beta(T_h - T_c)L^3}{\alpha\nu}, \text{Pr} = \frac{\nu}{\alpha}, \text{Pe} = \text{Re} \cdot \text{Pr} \quad (5)$$

where β is the thermal expansion coefficient, α is the thermal diffusivity, ν is the kinematic viscosity, T_h and T_c are for hot and cold wall temperature respectively.

A projection method, also known as a fractional step method, is used for the flow solver. This method is based on the Helmholtz-Hodge Decomposition Theorem (Chorin [4]), and detailed description of employment of projection method can be found in the work of Ramaswamy et al. [5].

3 Finite element formulations

Quadrilateral elements are used to discretize the problem domains. The Galerkin weighted residual method is used.

The variables V and T can be replaced by using the trial functions:



$$V(x, t) = \sum_{i=1}^n N_i(x) V_i(t) \quad (6)$$

$$T(x, t) = \sum_{i=1}^n N_i(x) T_i(t) \quad (7)$$

where x is the computational domain, i is the degree of freedom (DOF) index and n is the number of DOFs.

Under projection algorithms, the weighted residual forms of the momentum and energy equations can be written as (summation convention is implied)

Momentum:

$$\left(\int_{\Omega} N_i N_j d\Omega \right) \left\{ \dot{V}_i \right\} + \left(\int_{\Omega} N_i (N_k V_k) \frac{\partial N_j}{\partial x_j} d\Omega \right) \{V_i\} + \left(\int_{\Omega} \text{Pr} \frac{\partial N_i}{\partial x_i} \frac{\partial N_j}{\partial x_j} d\Omega \right) \{V_i\} - \int_{\Omega} f(x_i) N_i d\Omega - \int_{\Omega} C_{\text{visc}} N_i \frac{\partial N_j}{\partial x_j} \{V_i\} n_i d\Gamma = 0 \quad (8)$$

where Ω denotes (\mathbf{x}) and Γ represents the boundaries of the computational domain. For the vertical component (y) with natural convective effects:

$$f(x_i) = C_{\text{grav}} \{T_i\} = Ra \text{Pr} \{T_i\}$$

Energy:

$$\left(\int_{\Omega} N_i N_j d\Omega \right) \left\{ \dot{T}_i \right\} + \left(\int_{\Omega} N_i (N_k V_k) \frac{\partial N_j}{\partial x_j} d\Omega \right) \{T_i\} + \left(\int_{\Omega} \frac{\partial N_i}{\partial x_i} \frac{\partial N_j}{\partial x_j} d\Omega \right) \{T_i\} - \int_{\Omega} Q N_i d\Omega - \int_{\Omega} N_i q \Gamma d\Gamma = 0 \quad (9)$$

Equations (8) and (9) can be written in matrix form as

$$[M] \{\dot{V}\} + ([K_v] + [A(V)]) \{V\} = \{F_v\} \quad (10)$$

$$[M] \{\dot{T}\} + ([K_T] + [A(V)]) \{T\} = \{F_T\} \quad (11)$$

where the over dot refers to time differentiation. The matrix coefficients are defined as:

$$[M] = \int_{\Omega} N_i N_j d\Omega \quad (12)$$

$$A(V) = \int_{\Omega} N_i (N_k V_k) \frac{\partial N_j}{\partial x_j} d\Omega \quad (13)$$

$$[K_v] = \int_{\Omega} \text{Pr} \frac{\partial N_i}{\partial x_i} \frac{\partial N_j}{\partial x_j} d\Omega \quad (14)$$

$$[K_T] = \int_{\Omega} \frac{\partial N_i}{\partial x_i} \frac{\partial N_j}{\partial x_j} d\Omega \quad (15)$$

$$\{F_v\} = \int_{\Omega} N_i f(x_i) d\Omega + \int_{\Gamma} \text{Pr} N_i n_i \frac{\partial V_j}{\partial x_j} d\Gamma \quad (16)$$



$$\{F_T\} = \int_{\Omega} N_i Q d\Omega + \int_{\Gamma} N_i q d\Gamma \quad (17)$$

A Petrov-Galerkin scheme is employed to weight the advection terms in the governing equations. The altered weighting function skews the interpolation function in the upwind direction so that the dispersion and added diffusion introduced by the standard Galerkin formulation are minimized, i.e.

$$W_i = N_i + \frac{\hat{\alpha} h_e}{2|V|} [V \cdot \nabla N_i] \quad (18)$$

$$\hat{\alpha} = \coth \frac{\gamma}{2} - \frac{2}{\gamma} \quad (19)$$

where $\hat{\alpha}$ is the Petrov-Galerkin weighting factor, h_e is the characteristic element length and γ is the Petrov-Galerkin stability parameter. For flow with natural convection, $\gamma = |V| h_e Ra Pr$.

Mass lumping is used in order to obtain a fully explicit time marching scheme, i.e.

$$[M]^{-1} = 1/m_i \quad (20)$$

4 Adaptation methodology

4.1 Error estimator

Various error estimators exist that can be used in adaptation, e.g., the element residual method, interpolation methods, subdomain-residual methods, and projection method. The right chosen error estimator is the basis for a successful adaptation procedure. Detailed descriptions of different error estimators can be found in [6–9].

In this study, an error estimator was chosen based on an extension of the work by Zienkiewicz and Zhu [7] due to its reasonable accuracy, simplicity and ease of implementation. The errors in a finite element solution are the difference between the exact and approximate solutions, which can be expressed in certain norms such as the “Energy” norm or L_2 norm. In this simulation, the L_2 norm is adopted. The corresponding stress error measure can be written as

$$\|e_{\sigma}\| = \left(\int_{\Omega} e_{\sigma}^T e_{\sigma} d\Omega \right)^{1/2} \quad (21)$$

and all element errors are typically defined as:

$$\|e_{\sigma}\|^2 = \sum_{i=1}^m \|e_{\sigma}\|_i^2 \quad (22)$$

where m stands for the total number of elements.

The error indices $\eta = \eta_{\sigma}$ in the form of error percentage defined as:

$$\eta_{\sigma} = \left[\|e_{\sigma}\|^2 / \left(\|\sigma^*\|^2 + \|e_{\sigma}\|^2 \right) \right]^{1/2} \times 100\% \quad (23)$$



The error index η is used to guide the adaptation procedure. Temperature is set for the key adaptation variable in our paper.

4.2 Adaptation rules

4.2.1 Unstructured meshes, anisotropic and 1-irregular mesh adaptation rule for h -adaptation

An unstructured, anisotropic mesh is allowed which is an efficient, directional refined mesh where refinement in one directional is needed. The 1-Irregular mesh refinement rule allows an element to be refined only if its neighbors are at the same or higher level (1-Irregular mesh). By following this rule, multiple constrained nodes (parent node themselves are constraint nodes) can be avoided.

4.2.2 Minimum rule for p -adaptation

Hierarchical shape functions employed in p -adaptation can be categorized as: node functions, edge functions, face functions (for 3D cases) and bubble functions. The minimum rule states that the order for an edge common for two elements never exceeds orders of the neighboring middle nodes. For quadrilateral elements in 2D, both the horizontal and vertical orders must be considered.

4.2.3 hp constraints are employed to meet continuity requirements

As a combination of h - and p - adaptation, hp -adaptation can be either refined (unrefined) or enriched (unenriched) whenever necessary. The adaptation rules for h - and p - are combined in hp -adaptation. In addition, to maintain continuity of global basis function, constraints at the interface of elements supporting edge functions of different order are employed. The constraint represents a generalization of the hp -constraints, which is discussed in Demkowicz et al [10].

4.3 Adaptation strategy

An acceptable solution is reached when global and local error conditions are met. A global error condition states that the global percentage error should not be greater than a maximum specified percentage error: $\eta \leq \bar{\eta}_{\max}$. If $\eta > \bar{\eta}_{\max}$, a new iteration is performed. The local error condition states that local relative percentage error of any single element $\|e_{\sigma}\|_i$ should not be greater than the averaged error \bar{e}_{avg} among all the elements in the domain. The average element error is defined as:

$$\bar{e}_{\text{avg}} = \bar{\eta}_{\max} \left[\left(\|\sigma^*\|^2 + \|e_{\sigma}\|^2 \right) / m \right]^{1/2} \quad (24)$$

A local element refinement indicator $\xi_i = \|e\|_i / \bar{e}_{\text{avg}}$ is defined to decide if a local refinement for an element is needed: when $\xi_i > 1$, the element is refined; when $\xi_i < 1$ the element is unrefined.

In an h -adaptive process, the new element size is calculated using:

$$h_{\text{new}} = h_{\text{old}} / \xi_i^{1/p} \quad (25)$$



In a p -adaptive process, the new shape function order is calculated using:

$$p_{new} = p_{old} \xi_i^{1/p} \quad (26)$$

The hp -adaptive strategy used in this study employs a “ L_2 ” norm error estimator, which is an extension from the “three-step hp -adaptive strategy” developed by Oden et al. [11]. In the hp -adaptive procedure, a sequence of refinement steps is employed. Three consecutive hp -adaptive meshes are constructed for solving the system in order to reach a preset target error: initial mesh, the intermediate h -adaptive mesh, and the final hp -adaptive mesh obtained by applying p -adaptive enrichments on the intermediate mesh. The p -adaptation is carried out when the problem solution is pre-asymptotic.

5 Numerical results

5.1 Problem definition

Natural convection in a differentially heated cavity has been studied extensively for over 30 years (differentially heated vertical walls - hot left and cold right; adiabatic horizontal walls – top and bottom). Numerical simulation results are generally compared with the accurate benchmark solutions obtained by De Vahl Davis [12], who used a FDM with a stream function - vorticity formulation. In this study, the problem was solved using h -, p - and hp -adaptive FEM with $Pr = 0.71$, $Ra = 10^3 - 10^6$.

5.2 Simulation results

Results were obtained for $Ra = 10^3 - 10^6$. Excellent agreement was observed over the range of Ra numbers with data available in literatures [12]. Results from the lower Ra number computations are essentially duplicative with results found in the literature. Results for $Ra = 10^5$ and 10^6 are presented. Final adapted meshes and results for h -adaptation are shown in Figure 1. 3-level h -adaptation was employed and produced 2503 elements with 2542 DOFs for $Ra=10^5$.

Final adapted meshes and results for p -adaptation are shown in Figure 2. Only 3-level p -adaptation was used and created 400 elements with 1184 DOFs for $Ra=10^5$.

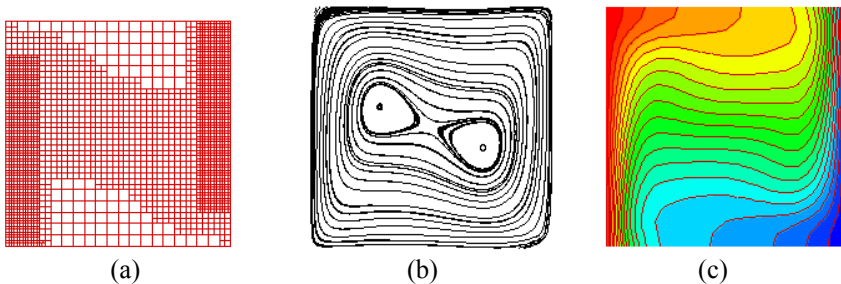


Figure 1: h -adaptive results for $Ra=10^5$ (a) final adapted mesh, (b) streamlines, and (c) temperature contours.

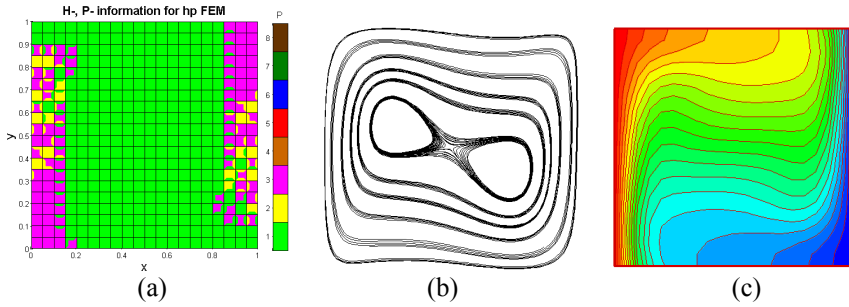


Figure 2: p -adaptive results for $Ra=10^5$ (a) final adapted mesh, (b) streamlines, and (c) temperature contours.

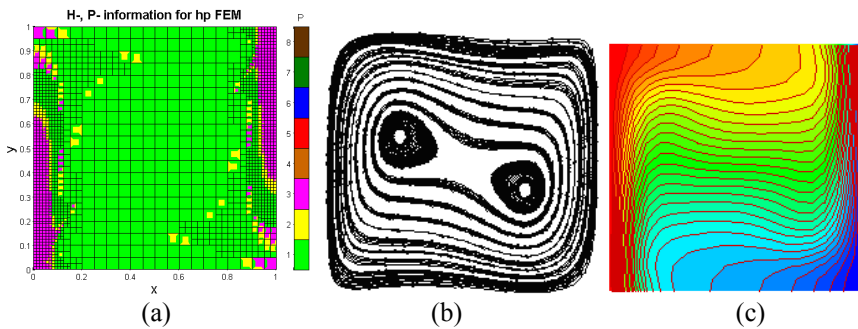


Figure 3: hp -adaptive results for $Ra=10^5$ (a) final adapted mesh, (b) streamlines, and (c) temperature contours.

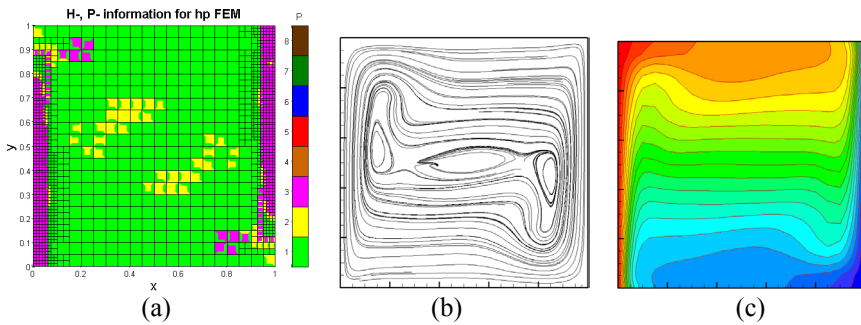


Figure 4: hp -adaptive results for $Ra=10^6$ (a) final adapted mesh, (b) streamlines, and (c) temperature contours.

Final adapted meshes and results for hp -adaptation are shown in Figures 3 and 5. In these simulations, both 3-level h - and p -adaptations were used resulting in 1368 elements and 6897 DOFs for $Ra=10^5$. The test case for $Ra=10^6$ produced a final mesh consisting of 1372 elements and 6529 DOFs, which is shown in Figure 4.

All the adaptive results agree well with benchmark data available in the literature for both flow and thermal patterns [12]. Quantitative studies were also conducted for the hp -adaptive algorithm with $Ra=10^6$. Comparisons with [12] were made for the maximum horizontal and vertical velocities together with their locations on the vertical and horizontal midplane; Nu_0 , the average Nusselt number on the heated wall; and the maximum and minimum values of local Nusselt number on the heated side together with their locations. Results of the comparison study are shown in Table 1.

6 Discussion

The adaptive algorithms change element size and shape function order dynamically. The adaptations are based on key variable gradients of the error distribution, subsequently producing highly accurate values with a minimum of computational cost. All three adaptive schemes are efficient in reducing overall computational time. This is particularly true for h -adaptation compared with a global uniformly refined algorithm. The p -adaptive algorithm is also effective when compared with a uniformly enriched algorithm. The hp -adaptive algorithm is the best of the three adaptive schemes, and has been shown to be exponentially convergent compared with uniformly refined and enriched techniques [13].

Table 1: Comparison of hp -FEM results with benchmark data ($Ra=10^6$).

	[12] results	hp -FEM results
u_{\max}	64.63	64.97
y ($x=0.5$)	0.850	0.890
v_{\max}	219.36	221.40
x ($y=0.5$)	0.0379	0.0381
Nu_0	8.817	8.672
Nu_{\max}	17.925	18.147
y ($x=0$)	0.037	0.042
Nu_{\min}	0.989	0.872
y ($x=0$)	1	1

A globally uniform h -refined and p -enriched mesh (uniformly refined up to 3-levels and enriched up to 3rd order) and the hp -adaptive algorithm (adaptively refined up to 3-levels and enriched up to 3rd order) were analyzed for $Ra = 10^5$. The initial mesh for the hp -adaptive algorithm was 10×10 . Results showed that using a globally h -refined and a p -enriched algorithm consumed nearly 18X more CPU time (projected) than the hp - adaptive algorithm, as shown in Table 2.

The choice of using a particularly type of adaptive algorithm and selection of key variables depends on various problem constraints and properties desired by the user. For example, a simple rectangular domain with simple boundary condition constraints can be solved without adaptation using conventional numerical methods. On the other hand, complex geometries and regions where



high gradients can occur are best handled using dynamic adaptive techniques – and eliminate the burden on the user of having to remesh the problem. A list of the advantages and disadvantages for each adaptive scheme is shown in Table 3.

Table 2: CPU time comparison between uniform refined and enriched algorithm and *hp*-adaptive algorithm.

Compare Cases	# of element		# of DOF		Total CPU Time	Per DOF CPU time	# of iteration
	Initial	Final	Initial	Final			
Uniform <i>h</i> and <i>p</i>	1600	1600	14641	14641	140,884 (sec)	9.62 (sec/DOF)	34500
<i>hp</i> -adaptive algorithm	100	436	121	1385	7741 (sec)	5.59 (sec/DOF)	35519

Table 3: Comparison of *h*-, *p*-, *r*- and *hp*- adaptive algorithm.

	<i>h</i> -adaptation	<i>p</i> -adaptation	<i>r</i> -adaptation	<i>hp</i> -adaptation
element size	various	constant	various	various
DOF (degrees of freedom)	various	various	constant	various
shape function	constant	various	constant	various
advantages	elements will not become overly distorted	relative coarse mesh may be sufficient	no new nodes added	exponential convergence rate
disadvantages	difficulty in dealing with constraint nodes	coding complexity	elements may become overly distorted	difficulty in dealing with constraint nodes and coding complexity

7 Conclusions

Three adaptive algorithms now being used in the finite element method have been developed to solve for fluid flow and heat transfer. Natural convection within a differentially heated enclosure was solved using *h*-, *p*- and *hp*-adaptive algorithms. Similar flow and thermal patterns were observed in all three adaptive solutions for $10^3 \leq Ra \leq 10^6$. Excellent agreement was obtained for all three methods compared with benchmark data available in the literature. Characteristics for the different adaptive algorithms are discussed. The



computational efficiency for the hp -adaptive algorithm showed an 18X decrease in CPU time compared to using a uniformly refined and enriched FEM algorithm. Adaptive algorithms are especially promising in dealing with problems where solution and error distributions are hard to predict.

References

- [1] Peraire J., Vahdati M., Morgan K., Zienkiewicz O.C., Adaptive Remeshing for Compressible Flows, *J. Comput. Physics*, 72 (2), pp26-37, 1987
- [2] Guo, B. and Babuska, I., The h - p Version of the Finite Element Method, Parts 1 and 2, *Comp. Mech.*, Vol. 1, pp. 21-21 and pp. 203-220, 1986.
- [3] Gui, W. and Babuska, I., The h , p and h - p Version of the Finite Element Method in One Dimension, Parts 1 and 2, *Numerische Mathematik* Vol. 49, pp.577-683, 1986.
- [4] Chorin, A. J., Numerical Solution of the Navier-Stokes Equations, *Math. Comp.*, Vol. 22, pp.745-762., 1968.
- [5] Ramaswamy, B., Jie, T. C. and Akin, J. E., Semi-Implicit and Explicit Finite Element Schemes for Coupled Fluid/Thermal Problems, *Int. J. Num. Meth. Engng.*, Vol. 34, pp.675-696., 1992.
- [6] P. Nithiarasu and O. C. Zienkiewicz, Adaptive mesh generation for fluid mechanics problems, *Int. J. Num. Meth. Engng.* 47, pp. 629-662, 2000.
- [7] Zienkiewicz O. C. and Zhu R. J. Z., A Simple Error Estimator and Adaptive Procedure for Practical Engineering Analysis, *Int. J. Num. Meth. Engng.*, Vol. 24, pp.337-357, 1987.
- [8] Oden, J. T., Demkowicz, L. Rachowicz, W. and Westermann T. A., Toward a Universal h - p Adaptive Finite Element Strategy, Part 2. A Posteriori Error Estimation, *Comp. Meth. Appl. Mech. and Engng.*, Vol. 77, pp.113-180, 1989.
- [9] Ainsworth, M. and Oden, J. T., *A Posteriori Error Estimation in Finite Element Analysis, Pure and Applied Mathematics*, A Wiley-Interscience Series of Texts, Monographs and Tracts, 2000.
- [10] Demkowicz, L, Oden, J. T., Rachowicz, W and Hardy, O, Toward a Universal h - p Adaptive Finite Element Strategy, Part 1. Constrained Approximation and Data Structures, *Comp. Meth. Appl. Mech. and Engng.*, Vol. 77, pp.79-112, 1989.
- [11] Oden, J. T., Wu, W. and Ainsworth, W., Three-Step h - p Adaptive Strategy for the Incompressible Navier-Stokes Equations, *Modeling, Mesh Generation, and Adaptive Numerical Methods for Partial Differential Equations*, Springer-Verlag, pp. 347-366, 1995.
- [12] De Vahl Davis, G., Natural Convection of Air in a Square Cavity: A Bench Mark Numerical Solution, *Int. J. Numerical Methods in Fluids*, Vol. 3, 249-264, 1983.
- [13] Wang, X. and Pepper, D. W., Application of an hp -adaptive technique for heat, mass and momentum transport, *ASME Int. Mech. Engng. Cong. and Exp.*, Nov.5-11, 2005 Orlando, Florida.

